El Cezeri
Journal of Science and Engineering
ISSN: 2148-3736

Research Article

A Study on Impatient Pedestrian Effect on Bi-directional Pedestrian Movement by Using Ant Algorithms

Tarık Kunduracı[1a]
[1]Department of Electricity and Energy, Manisa Celal Bayar University, Akhisar, Manisa,Türkiye
tarik.kunduraci@cbu.edu.tr

DOI : 10.31202/ecjse.1430803
Received: 02.02.2024 Accepted: 01.09.2024
How to cite this article:
Tarık Kunduracı, " A Study on Impatient Pedestrian Effect on Bi-directional Pedestrian Movement by Using Ant Algorithms", El-Cezeri Journal of Science and Engineering, Vol: 11, Iss: 3, (2024), pp.(327-337).
ORCID: [a]0000-0002-1854-1361.

Abstract : This paper aims to revisit the bidirectional walking of pedestrians to contribute to a more realistic definition of the case of the presence of impatient pedestrians and to depict the effect of including impatient walkers in the pure bi-directional system of ''normal'' walking pedestrians. It is found that when a trace amount of impatient pedestrians is added to the system, it affects traffic in a disruptive way at low densities, however, it affects constructively at medium and high densities interestingly. In addition, when adding a comparable amount of impatient pedestrians to the system, it is seen that at low and medium densities, the flux of motion and the order parameter change in parallel. In contrast, at high densities, the high number of impatient pedestrians positively affects lane formation, so pedestrian mobility remains high despite high density and disorder. As a result, more impatient pedestrians may not always mean more congested traffic. Sometimes, a certain density of impatient pedestrians can positively affect the bi-directional pedestrian traffic flow.

Keywords : Cellular Automata (CA), Computer Simulation, Bi-Directional Pedestrian Flow.

1 Introduction

In the literature, pedestrian dynamics have been investigated using several methods. The most frequently used ones are the social force model (SFM), continuum model (CM), and cellular automaton model (CA). The SFM is based on Newtonian mechanics and is one of the well-known microscopic simulation models for describing pedestrian dynamics [1]–[7]. The model that describes specific situations, like arching, lane formation, clogging, and the faster-is-slower effect was first introduced by Helbing. One of the social insects, as known, are ants that communicate with each other by a hormone called pheromone while they forage for food. Recently, it was shown that human travel behaviors seem to carry some similarities with those of ants [8]. So, one can use the ant communication path in the pedestrian movement in such a manner that each person will drop a ''visual pheromone'' to communicate with other ones [9]–[11]. As known, the pheromone dropped by an ant evaporates with time. Similarly, our visual pheromone does the same: The commonly preferred routes will be preferred again with a great probability by pedestrians as we know our daily observations. This means that the visual pheromone will be refreshed if pedestrians keep using the same routes. The non-preferred or less preferred ones will vanish due to evaporating of the visual pheromone. As an example, for this analogy, the collective behavior of other biological entities to design a safe evacuation scenario has been studied in the literature: a mathematical model is proposed based on the approach that is used to describe animal dynamics to simulate the collective traffic [12], [13] .

Some ant species, for example, Pharaoh's ants drop repelling pheromone to warn others that there is no entry [14]. This keeps other forager ants away from unrewarding paths. The lane formation phenomenon in pedestrian movement includes two behavioral elements known as ''following'' and ''avoidance'' that may correspond to the visually attractive and repellent pheromones, respectively [15], [16].

In literature, a theoretical model for ant trail traffic was studied including two distinct types of ant species one of which ''smells'' reasonably good than the other [17]. The flux vs evaporation rate of pheromone was investigated comprehensively. In another study, the traffic on a unidirectional ant trail was investigated theoretically on the base of CA by mixing good-smelling and poor-smelling ants on the trail. In the study, ants were thought of as vehicles that travel, and TASEP (Totally Asymmetric Simple Exclusion Principle) was employed, known as Nagel-Schreckenberg Model (NaSch Model) in traffic modeling [18]. In addition, the unidirectional ant traffic flows with a U-turn in an ant trail was studied by using a one-dimensional CA model [19], [20].

All these similarities between movement rules given above have been a motivating point to examine the bi-directional pedestrian

traffic by imposing ant algorithm. A study has been done in this context where pedestrians decide to move according to the amount of visual pheromone. The movement probabilities are calculated as a function of repellent and attractive pheromones. This work is an extended version of the study performed earlier [21]. All the movement rules in this reference are valid, but in this study, all pedestrians are not identical, some of those are ''impatient'' and tend to move two times faster. A similar study has been done very recently, in which the Kinetic Monte Carlo method was employed [22]. In there, the bi-directional pedestrian flows with different walk speeds are studied in the CA context choosing Moore neighborhoods. Very recent studies, ''the phase behaviors of counterflowing stream of pedestrians'' and, ''the pedestrian evacuation model of impatient queueing'' have been examined, respectively [23], [24].

2 The Model

The system is constructed as a two-dimensional cell grid with the size of $L \times L$, where L defines here system size. In the work, L is taken as 50. The cells may be occupied by just one pedestrian or may be empty. All pedestrians move synchronously in a time step. If a pedestrian is an ''impatient'' one and if there are two empty cells in his/her neighborhood then he/she is permitted to move double cells per time step, which may be introduced as an extension of Von Neumann neighborhood[1], else he/she obeys ordinary Von Neumann neighborhood rules of motion in CA (Fig.1). Moving backward is not allowed. The simulations are

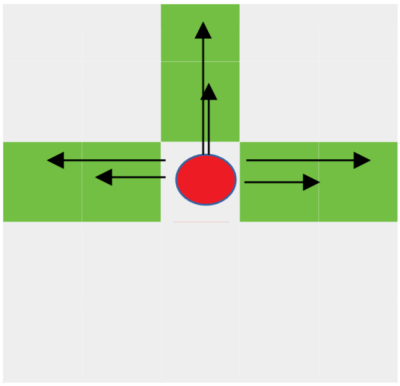

Figure 1: An extended version of Von Neumann neighborhood for a pedestrian who is represented as a red full circle. The green cells are empty, and the pedestrian can move to them in next time step.

performed in a square corridor, which is populated by two species of pedestrians, i.e., the top-down walkers and the bottom-up walkers who also include the ''impatient'' population (Fig. 2). The numbers of top-down and bottom-up walkers are set to be equal. At initial, they are randomly distributed in the corridor. The periodic boundary conditions are applied at the bottom and the top boundaries. While the top-down walkers arrive at the bottom, they continue the movement and enter the corridor from the upper boundary. When the bottom-up walkers arrive at the top boundary, they continue to move and enter the corridor from the bottom boundary. The right and left boundaries are assumed to be walls, so pedestrians are not allowed to cross; the closure boundary conditions are applied to the right and left boundaries. The colored arrows shown in Fig. 2 represent pedestrians

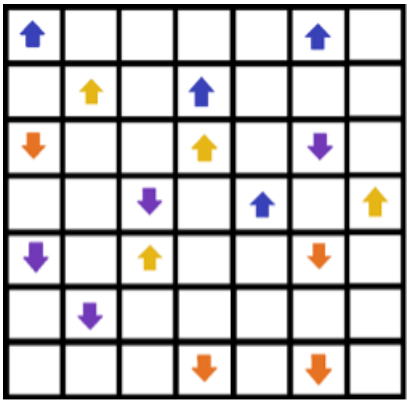

Figure 2: A Schematic diagram to illustrate the bottom-up and top-down walkers in two opposite main directions (south-north and north-south). The different colored arrows stand to distinguish the impatient pedestrians.

1. A discussion about the extended version of Von Neumann and Moore neighborhoods can be found in [25].

Table 1: The bottom-up walker updating rules. The dark cells are occupied. The impatient walker prefers to move with $v_{max} = 2$ if the neighboring two adjacent cells are empty; if not, it obeys the updating rules corresponding to the ordinary Von Neumann neighboring ($v_{max} = 1$). The top-down walker updating rules, which are not presented here, are the same but the reverse movement direction must be held.

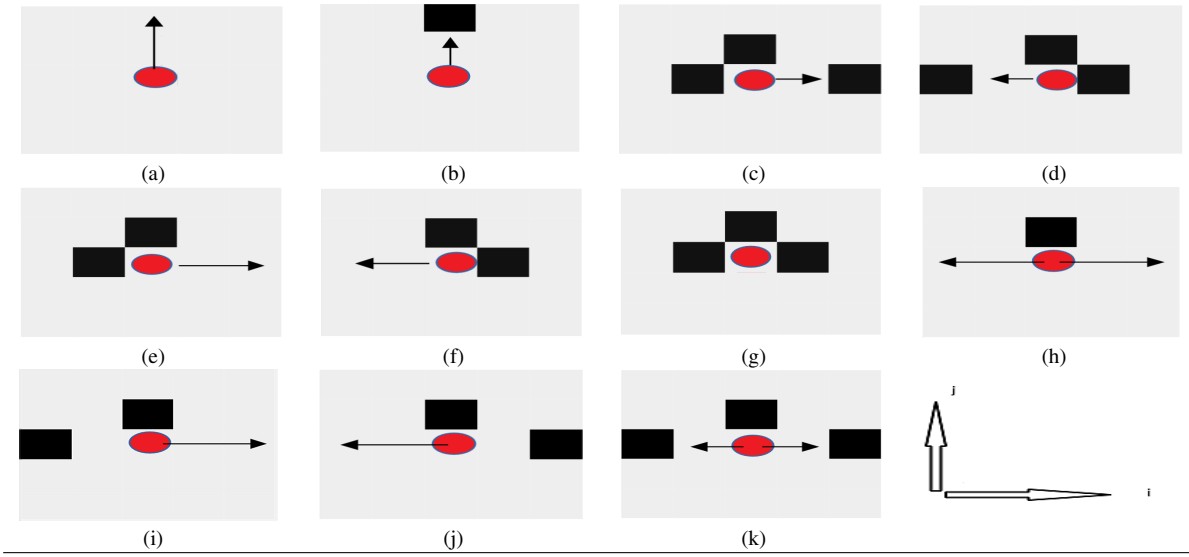

moving in two specific directions i.e., south-north and north-south. In the south-north direction, the bottom-up walkers are represented by yellow-and blue-colored arrows, whereas in the north-south direction, the top-down walkers are represented by orange- and purple-colored arrows. Yellow arrows stand for patient bottom-up walkers while blue ones stand for impatient bottom-up walkers, conversely, orange arrows stand for top-down patient walkers while purple arrows for top-down impatient walkers. All pedestrians/walkers are assumed to drop visual pheromones according to the direction they move. The pheromone dropped from a bottom-up walker is attractive for the same kind of walker but is repellent for a top-down walker, and vice versa.

At each time step, the update of the state of the system is carried out synchronously in two stages, as follows: In the first stage, all the pedestrians are sequentially moved by imposing the rules that have been mentioned above, and the new configuration $(W(t+1), p(t+1))$ is composed of the old configuration $(W(t), p(t))$ at time t, where W and p refer to pedestrian and pheromone states, respectively. In the second stage, the pheromone is allowed to evaporate for updating of $p(t)$.

The updating rules are given in Table1 for a bottom-up walking pedestrian. In the table, an impatient bottom-up walker moves to another cell according to the updating rule corresponding to the extended Von Neumann neighborhood. This updating rule is one of the updating rules of the Nagel-Schreckenberg traffic model with $v_{max} = 2$ [18], [21]. The impatient bottom-up walker primarily prefersto move to the second neighboring cell in front (Table 1(a)), if the first and second two adjacent neighboring cells in front are simultaneously empty. Namely, a transformation, when

$$t \to t+1; (W_{i,j}(t) = 1, W_{i+2,j}(t) = 0) \to (W_{i,j}(t+1) = 0, W_{i+2,j}(t+1) = 1)$$

takes place with a probability where i,j refer to the coordinates of the current cell. If a cell is empty at time t, the state of the cell is $W_{i,j}(t) = 0$ or if occupied by a pedestrian, it is $W_{i,j}(t) = 1$. The bottom-up walker may also move right and left neighboring empty cells if the up-neighboring cell is occupied at time t, which means the transformation

$$(W_{i,j}(t) = 1, W_{i\pm2,j}(t) = 0) \to (W_{i,j}(t+1) = 0, W_{i\pm2,j}(t+1) = 1)$$

takes place with a probability as $t \to t+1$(Table 1(h)). In cases (i) and (j), it is seen that the bottom-up walker makes the decision likely to move to the side where the two adjacent empty cells exist. If only one neighboring cell is empty as shown in cases (e) and (f) in Table 1, the walker moves to the empty cell with a probability. In (e) and (f), the second neighboring empty cell is visited with a probability if two adjacent left/right cells are empty at time t. The probability of the movement is determined fully by the visual pheromone concentration left by pedestrians in cells. The net pheromone concentration is obtained by subtracting pheromone 2 from pheromone 1, where pheromones 1 and 2 indicate attractive and repellent visual pheromones, respectively. Namely,

$$ph_{net} = ph_1 - ph_2 \tag{1}$$

For both walker types, the first pheromone i.e., pheromone 1 is attractive and pheromone 2 is *repellent*. That is, when investigating the movement of the bottom-up walkers, pheromone 1 belongs to the bottom-up walkers and pheromone 2 to

the top-down walkers, but when investigating the movement of the top-down walkers, pheromone 1 belongs to the top-down walkers and pheromone 2 to the bottom-up walkers. Pheromone concentrations are chosen as 0.0, 0.5, and 1.0. Thus, the net pheromone may be negative, meaning that it is not permitted to move, and if it equals 0.0 the probability to move is only 5%.

Table 2: Movement probabilities according to the net pheromone concentration in a cell.

ph_{net}	Probability to move
< 0	0.00
=0.0	0.05
+ 0.5	0.15
+ 1.0	0.80

In Table 2, all the movement probabilities are given. It seems that the most probable motion occurs when the net pheromone

Table 3: The visual pheromone updating rules. When a cell is occupied by a pedestrian at the end of the first stage, a pheromone is leaved. If the cell is empty, the pheromone concentration will gradually decrease by 0.5 with the probability f.

Probability of Evaporation	$W_{i,j}(t+1)$	$p_{i,j}(t)$	$p_{i,j}(t+1)$
$-$	1	1.0	1.0
$1-f$	0	1.0	1.0
f	0	1.0	0.5
$1-f$	0	0.5	0.5
f	0	0.5	0.0

concentration is $+1.0$ in a cell. When the concentration is $+0.5$, the probability of motion for a walker decreases to 15%. Pheromones evaporate over time, thus in a cell, the concentration of pheromone decreases with the evaporation rate f which is also a probability and $f ?[0,1]$. If a cell is occupied by a pedestrian then the pheromone concentration is set to 1.0 for all types at the end of the first stage, namely if $W_{i,j}(t+1) = 1$ then $p_{i,j}(t+1) = 1.0$. But, if the cell is empty i.e., $W_{i,j}(t+1) = 0$ then the pheromone concentration decreases with the probability of evaporation. The pheromone updating rules are summarized in Table 3.

3 The Order Parameter and Flux and Velocity

The order parameter is a useful value that enables us to follow a system ordering degree. The evolution of a stochastic system can be followed by a few parameter sets; for example, the order parameter and the flux of the system. To calculate the order parameter, it is proposed to use, [15], [21], [26]

$$\phi_n = \left[\frac{N_{jn}\uparrow - N_{jn}\downarrow}{N_{jn}\uparrow + N_{jn}\downarrow}\right]^2 \tag{2}$$

where N_{jn}^{up} and N_{jn}^{down} stand for the number of bottom-up and top-down walkers at the corresponding column, *jn* respectively. The calculation is performed over the column *jn*. Then the global order parameter Φ is calculated over all pedestrians from the formula

$$\Phi = \frac{1}{N}\sum_{n=1}^{N}\phi_n, \tag{3}$$

where ϕ_n is being individual order parameter described in Eq.(2) and N is the number of whole pedestrians.

Another parameter is the flux of the movement defined as $< J >= \rho < v >$ where $< v >$ is the total velocity calculated over the Metropolis Monte Carlo (MMC) cycles as an average can carry important information about the phase transformation points of the bi-directional system. Also, the speed of the walkers v is known as one of the features of pedestrian traffic. Indeed, the velocity and flux for top-down and bottom-up walkers are calculated separately (without distinguishing as patient-impatient) as $v\uparrow = N\uparrow /N$, $v\downarrow = N\downarrow /N$ and $J\uparrow, J\downarrow$, respectively. Then, the total velocity is calculated as

$$< v >= (N\uparrow + N\downarrow)/N \tag{4}$$

and the total flux is calculated as

$$< J >= (N\uparrow + N\downarrow)/L^2, \tag{5}$$

where $\rho = N/L^2$. In the following section, these observables are calculated as the average values over the Metropolis Monte Carlo (MMC) cycles for studying the pedestrian movement where half of the walkers are let walk from the top to the bottom and vice versa.

4 Results and Discussion

In this section, the results of the MMC simulations are given. In each simulation, the data is taken after 2×10^5 MMC cycles and the system is assumed to reach equilibria in which all the mentioned observables has no longer large fluctuations. The results are given in two sections: In the first section, the bi-directional walking system is simulated so that the impatient pedestrian population number is set fairly low. In the beginning, the system consists of a pure patient pedestrian population. Then, a trace amount of the impatient pedestrian population is added increasingly at every three stages which are explained below. In the second section, simulations are performed with comparable amounts of the impatient pedestrian population. This population is added to the bi-directional walking system at two stages. In the first stage, the impatient pedestrian population size is selected as small, while the patient pedestrian population size is selected as large. Subsequently, in the second stage, these population amounts are exchanged.

4.1 Adding Trace Amount of the Impatient Pedestrians (ImP) to the Bi-Directional Pedestrian Movement

Firstly, it is aimed to study how pedestrian walking behavior is affected by ''adding'' a few ''impatient'' walkers labeled as ImP into both walking directions. The patient pedestrians walking at normal or average speed are labeled as PaP. If there is no ImP as a walker in the system, this state is labeled as the initial pure state of the system. In the pure state, where all pedestrians are patient (PaP), the situation is equivalent to that of in [21] except for some rules, therefore the simulation results have similar patterns.

If a certain amount of ImP is added, the system has an impure state. The inserted ImP walkers affect the system so that the observed phenomena such as ''faster is slower'' and ''lane formation'' in the initial pure state are deformed. The simulations are reperformed in each case and, the average values of observables (velocity, flux, and order parameter) are calculated over the last 10^3 MC cycles. In Fig. 3, the order parameter Φ_0 that changes by the density ρ and evaporation rate f is given. The subscript ''0'' in Φ_0 and in J_0 stands for indicating the pure state where no ImP does exist.

- **Inserting ImP as 1% of patient pedestrians (PaP)**: In this case, a few numbers of walkers that make 1% of PaP are inserted as ''impatient walkers (ImP)'' into the system to create impurity in the pedestrian walking. This is similar to ''introducing impurities'' in a pure crystal structure to alter the conducting properties. In an oppositely walking pedestrian system, the amount of flux may correspond to the conductivity or resistivity of a semiconductor. The order parameter here is Φ_1, and the flux is J_1.
- **Inserting ImP as 2% of patient pedestrians (PaP)**: As in the previous case, 2% of PaP is inserted as ImP into the system to simulate. The rate is now two times bigger. The 3^{rd} row in Fig. 3, the change of the order parameter Φ_2 and flux J_2 vs. the density ρ are given.
- **Inserting ImP as 4% of patient pedestrians (PaP)**: In the last case, ImP is 4% of PaP. In the last row of Fig. 3, the simulation results for order parameter and flux are plotted vs. the density ρ.

It is seen from Fig. 3 that a discontinuous phase transition at $\rho \approx 0.30$ for $f = 0.01$ (red-colored) and for all percentage values of ImP has been clearly observed. This means that the transition does not depend on the change of the percentage of ImP, but depends on the change of f, which pertains to the motivation level to move. Moreover, the order parameters Φ_k and fluxes $J_k, (n = 1, 2, 4)$ both decrease smoothly for each fixed f value smaller than 0.01, which indicates second-order phase transitions. All transitions that occur take place from the ordered phase to the disordered phase. The less f value does not always result in more flux or mobility of the pedestrians, contrarily, it is observed from the simulations that it causes congestion in the bi-directional motion. The decomposition of the order parameters is less because contributions of regular flow on the remaining lanes to the order parameter still exist. Some snapshots in Fig. 4 are given, where the colored small squares represent pedestrians moving. Results shown in Figs. (4-8) are done by averaging over the last 10^3 MMC simulation cycles. The orange squares are bottom-up walkers and the light brown squares are top-down walkers, as shown in (a), (c), and (e) parts of the figure, where no ImP exists. In (b), (d), and (f), ImP is added to the motion as 1% of PaP. In each case, the simulation starts at the beginning. The ImP are colored purple for bottom-up walkers and burgundy for top-down, respectively. The walls of the corridor are colorized yellow and the empty squares are seen as black. The evaporation rate is taken as $f = 0.0001$.

The first two snapshots of Fig. 4 belong to the case that $\rho = 0.13$ and $N = 300$. For the Fig. 4(a), the lanes are seen in both directions in the corridor. The total flux J_1 calculated is 0.0017 and the average velocity v is 0.63 where $\Phi_1 = 0.78$. When 1% of N is added, the number of lanes decreases, and some small clusters appear as seen in 4(b). And flux, velocity, and order parameters both decrease to the values $J_1 = 0.0013$, $v = 0.57$, and $\Phi_1 = 0.57$ respectively. In 4(c) the density is $\rho = 0.21$ and $N = 500$ where $J_1 = 0.0012$, $v = 0.36$ and $\Phi_1 = 0.44$. The values surprisingly increase when $N \rightarrow (1 + 1\%)N$ is held. The situation is shown in 4(d). The new values are $J_1 = 0.0019$, $v = 0.49$, and $\Phi_1 = 0.47$, respectively. It is observed that the number of lanes doesn?t change but that of clusters decreases and the size of those becomes narrower. This makes a positive contribution to the traffic flow in the system in both directions.

In the first part of the last snapshots of Fig. 4, where $\rho = 0.39$ and $N = 900$, an aggregation formed by the bottom-up walkers

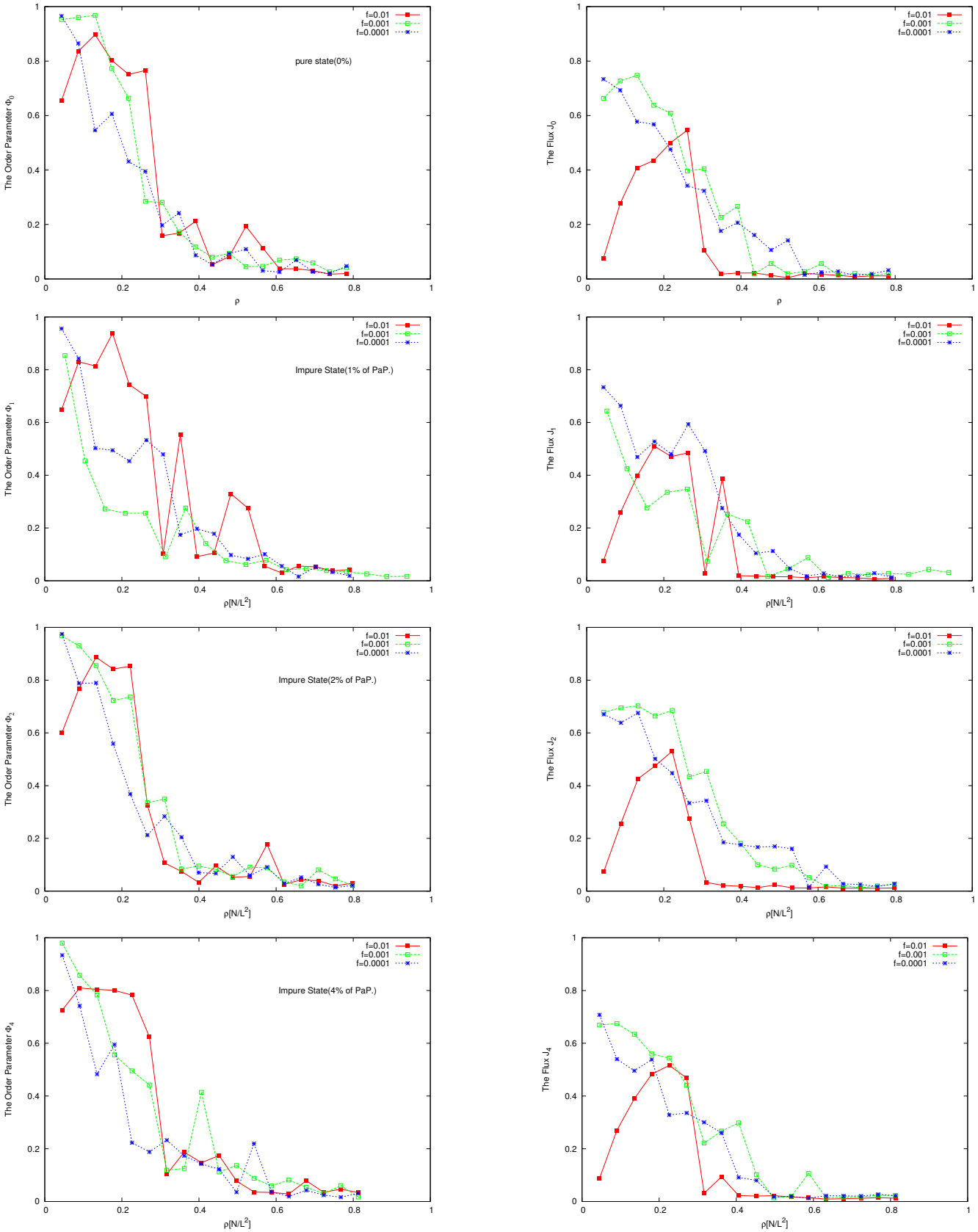

Figure 3: When the impatient walkers (ImP) are inserted into the system. The Order Parameter Φ_k and the flux J_k vs. ρ with different f values. The subscripts indicate the percentage of ImP.

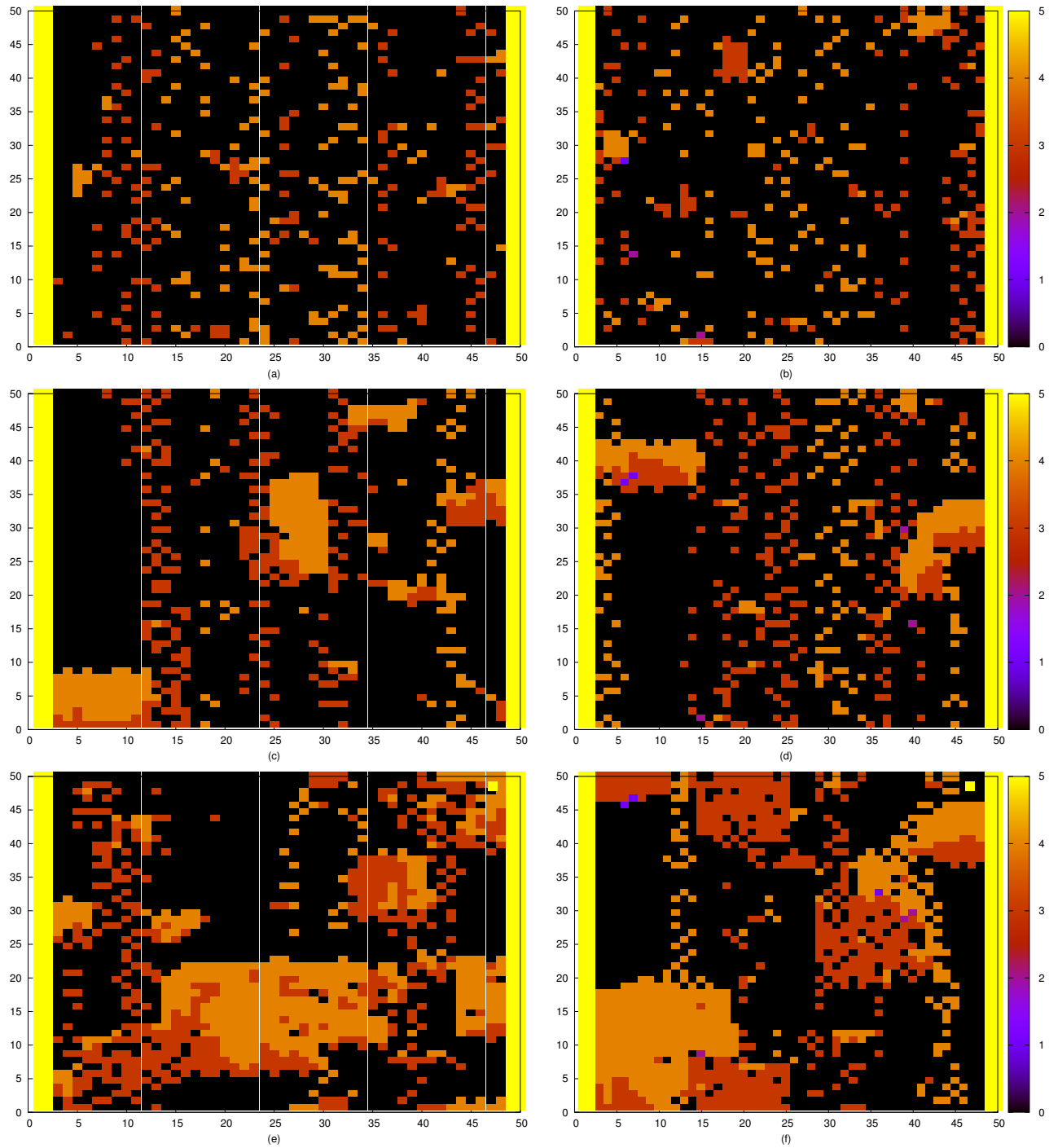

Figure 4: Some snapshots about the trace amount of ImP where $f = 0.0001$ is taken. The bottom-up walkers are colored by orange and the top-down walkers by light brown. In all cases, half of the population walks oppositely: $N/2 \uparrow, N/2 \downarrow$.

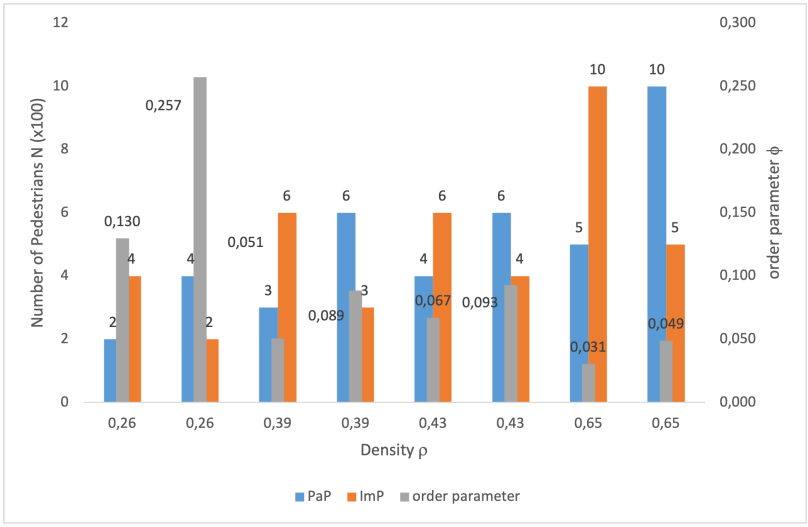

Figure 5: The total pedestrian number is set to $N = 600, 900, 1000$, and 1500, respectively where $f = 0.001$. There are four successive bar groups illustrated for the case when a comparable amount of ImP is added.

colored by orange is seen in the corridor. This leads to big congestion. In addition, some partially formed lanes and some cluster formations are observed. In this case, the observables are as follows: total flux is $J_1 = 0.0012$, the average velocity $v = 0.27$, and the order parameter is found as $\Phi_1 = 0.23$. The second part (i.e., 4(f)) includes slightly different patterns giving those observables as $J_1 = 0.0013$, $v = 0.28$, and $\Phi_1 = 0.35$. As seen, there is no remarkable change in flux and velocity, but the order parameter increases fairly, most likely, due to the disappeared blockage when the transformation $N \to (1 + 1\%)N$ holds. Similarly, at other ratios (2% and 4) the simulations give roughly the same results as understood while looking at Fig. 3. All those studies show that such a few ImP addition into a system including a large number of "normal-speeded" pedestrians (PaP) affects traffic in a disruptive way at low densities, however, it affects constructively at middle and high densities, interestingly.

4.2 Adding Comparable Amount of ImP to the Pedestrian Bi-Directional Movement

Secondly, the simulation of the bi-directional motion of the walkers including comparable amounts of PaP and ImP has been studied. In this subsection, the number of total pedestrian N is selected arbitrarily as $600, 900, 1000$, and 1500, respectively, and $f = 0.001$. There are exactly four cases for each density as shown in Fig. 5. Here, a condition is made. The condition is that the sum of the number of PaP N_P and the number of ImP N_I equals N which remains constant in each case, where N_P and N_I are chosen reciprocally unequal. In the first situation, N_P is large which means that the PaP population dominates over the ImP population ($(N_P > N_I)$), and vice versa in the second: ($(N_P < N_I)$). Simulations for each case aim to determine how the movement of walkers walking oppositely is affected under this population size condition. To show this situation, Fig. 5 is constructed.

In the figure, there are four successive bar groups each of which stands for distinct population size and density and are colorized blue and orange. At the top of each bar, N_P and N_I are given. The order parameter values Φ's are given at the corresponding grey narrower bars. For example, for $\rho = 0.26$, there are two bar groups colorized. The blue bar in the first group indicates the number of PaP as $N_P = 200$ and the orange bar indicates the number of ImP as$N_P = 400$. In the second group, the blue bar indicates again the number of PaP but as $N_P = 400$, and the orange one indicates again the number of ImP but this time as $N_I = 200$. It seems that the order parameter Φ takes 0.130 at first and increases then to $\Phi = 0.257$ as the values N_P and N_I are exchanged.

The same procedure is valid for other cases as well. The second case is for $\rho = 0.39$ where $N = 900$. In this case, $N_P = 300$ and $N_I = 600$ and the corresponding order parameter equals 0.051. The order parameter takes the value $\Phi = 0.089$ when the values of N_P and N_I are exchanged and take values 600 and 300. In the third and fourth cases, as in the previous two cases, it was observed that the order parameter gets higher values when $N_P < N_I \to N_P > N_I$ holds. That is when the population of ImP is low relative to that of PaP or, in other words, the population of PaP is high concerning that of ImP, the order parameter has been found to take high values. This means that a large population of ImP leads to a less ordered system than a system that dominates with PaP.

The same procedure is valid for other cases as well. The second case is for $\rho = 0.39$ where $N = 900$. In this case, $N_P = 300$ and $N_I = 600$ and the corresponding order parameter equals 0.051. The order parameter takes the value $\Phi = 0.089$ when the values of N_P and N_I are exchanged and take values 600 and 300. In the third and fourth cases, as in the previous two cases, it was observed that the order parameter gets higher values when $N_P < N_I \to N_P > N_I$ holds. That is when the population of ImP is

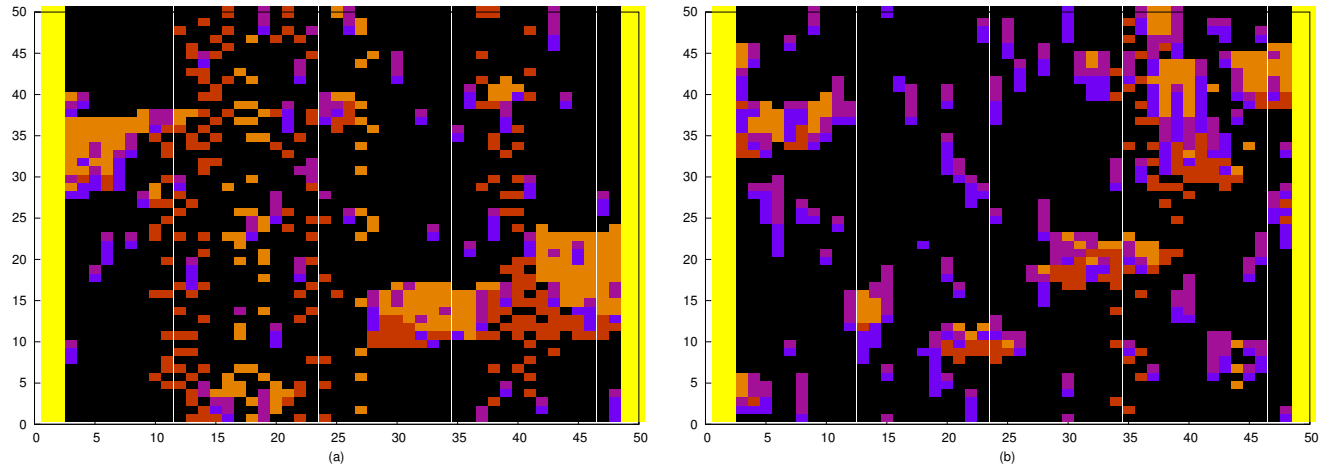

Figure 6: The snapshots of the simulation of bottom-up and top-down walkers at a square corridor with $L = 50$. Here, $N = N_P + N_I = 600$, $\rho = 0.26$, and f is 0.001. In all cases, half of walkers walk oppositely: $N/2 \uparrow, N/2 \downarrow$. The ImP part of bottom-up walkers are colored by purple while the PaP part of those are colored by orange, however, the ImP part of top-down walkers are colored by burgundy while PaP part of those are colored by light brown.

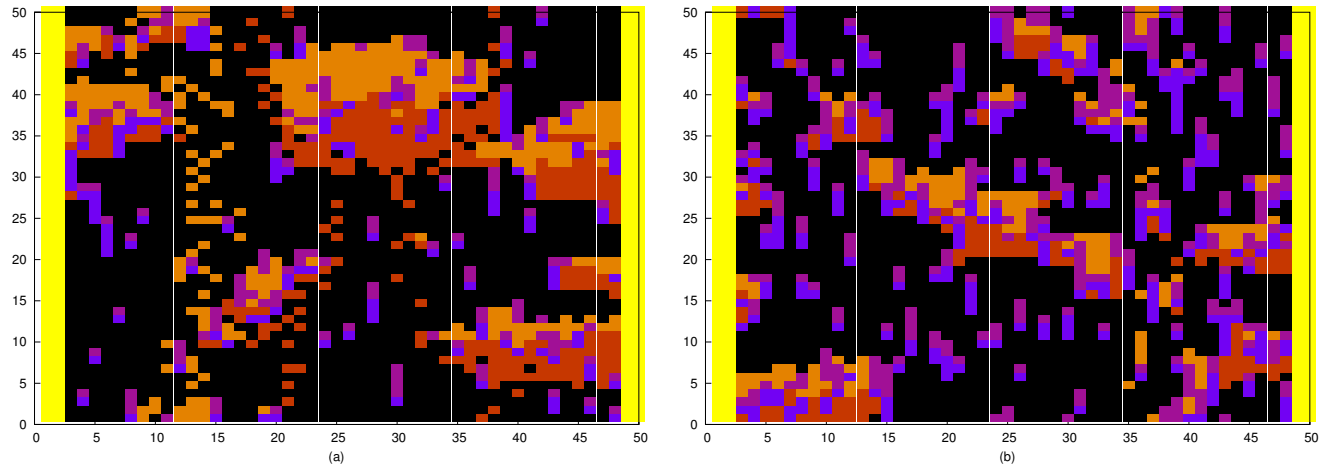

Figure 7: Another snapshot of the simulation of bottom-up and top-down walkers at a square corridor with $L = 50$. Here, $N = N_P + N_I = 900$, $\rho = 0.39$ and $f = 0.001$. In all cases, half of the populations walk oppositely: $N/2 \uparrow, N/2 \downarrow$. The colorizing rules are also the same as in Fig. 6.

low relative to that of PaP or, in other words, the population of PaP is high concerning that of ImP, the order parameter has been found to take high values. This means that a large population of ImP leads to a less ordered system than a system that dominates with PaP. The first snapshots of the simulation of this movement are given in Fig. 6. Here, results are done by averaging over the last 10^3 MC simulation cycles as mentioned before. The ImP part of the bottom-up walkers is colored purple while the PaP part of those is colored orange, however, the ImP part of the top-down walkers is colored burgundy while the PaP part of those is colored light brown. In the figure, the total pedestrian number is set to $N = 600$ thus, the density of pedestrians equals 0.26 and $f = 0.001$. In the first case (a), where the number of PaP is taken as $N_P = 400$ and the number of ImP $N_I = 200$, the lanes built by the bottom-up and top-down part of PaP are clearly seen, where $\Phi = 0.257$ and flux is $J = 0.275$. In (b), where $N_P \leftrightarrow N_I$ exchange is made, both Φ and J get lower values and local clusters emerge in some parts of the corridor: $\Phi = 0.129$ and flux is $J = 0.071$. In Fig. 7, snapshots of MC simulation of the bottom-up and the top-down walkers at a square corridor are given. The deformations of the lane formations are seen. In (a), $N_P > N_I$ and $\Phi = 0.089$, lanes produced by PaP for both walker types colored light brown and orange are observed. And also, some small full lanes consisting of ImP that intercept mutually each other's walk are seen. Here, the flux of the movement is computed as $J = 0.150$. In (b), on the contrary, $N_P < N_I$ and $\Phi = 0.051$, lower than the previous case. The lanes produced by PaP disappear but small ones remain, which give rise to a crowd at about the center of the corridor. The flux computed is $J = 0.036$, which is significantly lower. The snapshots for $\rho = 0.43$ and $N = 1000$ are given in Fig. 8. In 8(a), lane formations are almost gone relative to Figs. 6 and 7, but a few remain, and a big

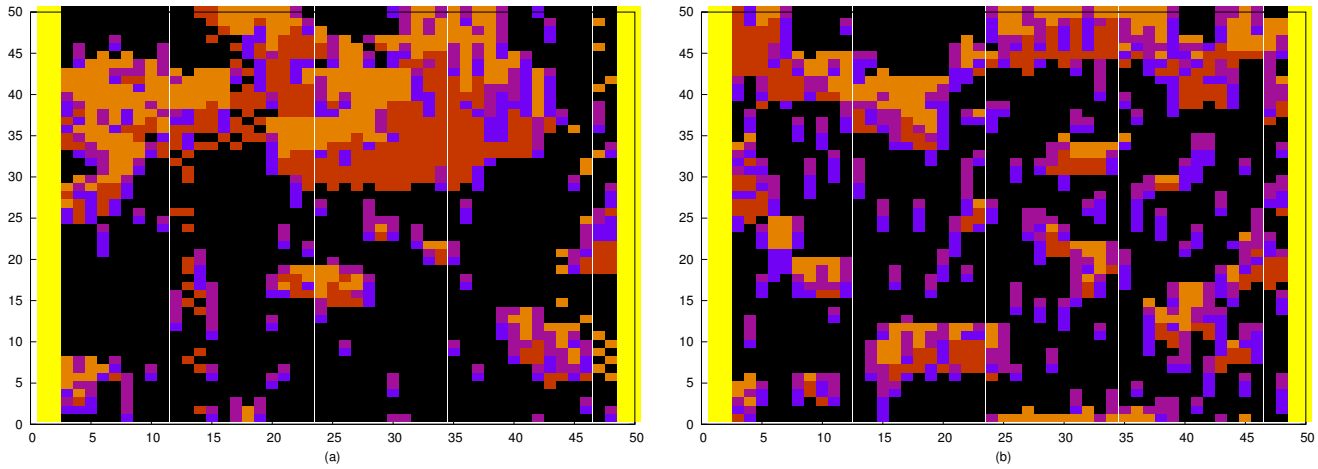

Figure 8: Other snapshots of the simulation of bottom-up and top-down walkers at a square corridor with $L = 50$. Here, $N = N_P + N_I = 1000$, $\rho = 0.43$ and f is the same. The colorizing rules are also the same as in Fig. 6. In all cases, half of the populations walk oppositely: $N/2 \uparrow, N/2 \downarrow$.

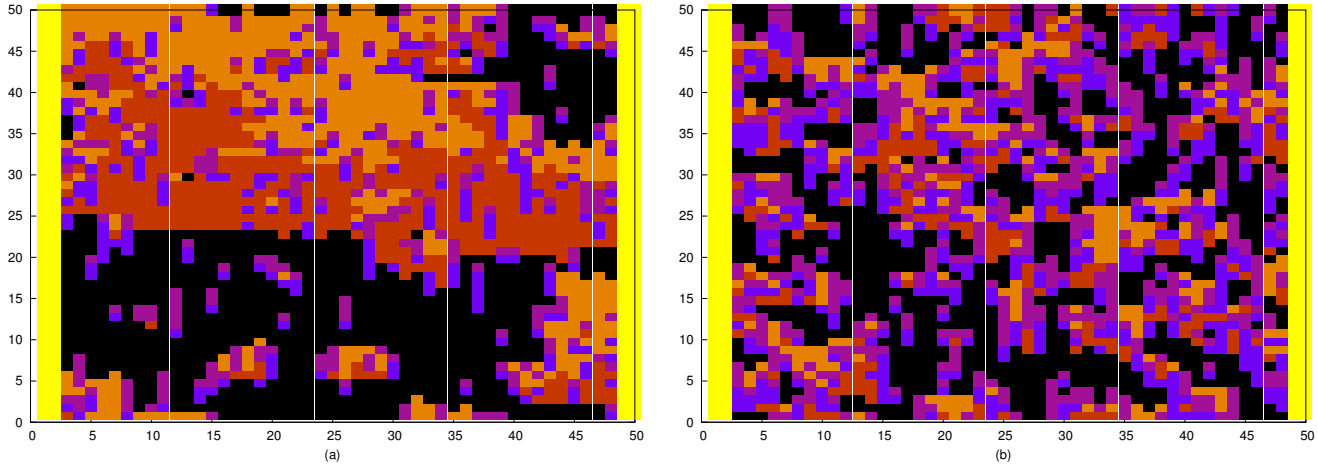

Figure 9: The last snapshots of the simulation of bottom-up and top-down walkers at a square corridor with $L = 50$. Here, $N = N_P + N_I = 1500$, $\rho = 0.65$ and f is the same. The colorizing rules are also the same as in Fig. 6. In all cases, half of the populations walk oppositely: $N/2 \uparrow, N/2 \downarrow$.

cluster caused by PaP is seen on the north side of the corridor. The ImP are seen as responsible for this cluster because they force the PaP to come together. In 8(b), after the exchange of pedestrian numbers, it is seen that the cluster becomes narrower and spreads out due to the existence of more ImPs who block mutually each other. The last snapshots of the bi-directional walkers' simulation are given in Fig. 9, where the total number of pedestrians is the largest: $N = 1500$. The density ρ is 0.65 and the average speed of walkers along the corridor, unlike the previous ones, almost vanishes. In the first case (a), the number of PaP is larger than that of ImP: $N_P = 1000, N_I = 500$. A crowd, causing congestion is obviously observed along the north side of the corridor, produced by the top-down and the bottom-up walkers of PaP. Also, the walkers of ImP block themselves oppositely along the corridor. All these together point out a jammed phase. In case (b), surprisingly, the crowd disappears and clusters produced by burgundy and purple walkers remain, who are impatient. Another conclusion is that, although the system order decreases ($\Phi : 0.049 \rightarrow 0.030$) by taking large number of ImP, the flux increases ($J : 0.013 \rightarrow 0.029$). This happens probably due to the termination of the huge cluster appeared in (a) after exchanging pedestrian numbers of PaP and ImP. This leads to relatively high pedestrian mobility alongside the corridor which means that after the exchange of numbers, an increase in the mobility (emerging in the flux) is due to the new lane formations made by the ImP.

5 Conclusion

This work aims to study the effect of the ‘‘modified’’ agents on the bi-directional walking system in general when the interacting item is a ‘‘visual pheromone’’ that is assumed as the communication tool between humans [8]–[11]. The Metropolis Monte

Carlo (MMC) simulation method with $v_{max} = 2$ as hopping speed is performed. The modified Von Neumann neighborhood is preferred. In this study, the modified agents are considered impatient pedestrians beside the patient pedestrians in the walking system. It is found that when a trace amount of impatient pedestrians are added to the system, some remarkable differences in fundamental patterns of pedestrian traffic have been observed with the help of the general observables such as flux and order parameters. In particular, a few ImP additions into a system including a large number of ''normal speeded'' pedestrian (PaP) affects traffic in a disruptive way at low densities. However, it affects constructively at middle and high densities interestingly. As an ambulance helps manage vehicle traffic in congested areas, some people in pedestrian traffic can play a constructive role in reordering the walking path.

When adding a comparable amount of impatient pedestrians to the bi-directional walking system it is seen that at low and middle densities, the flux of motion and the order parameter change in parallel. They both decrease while exchanging the number of patient and impatient pedestrians, i.e., while the transformation $N_P > N_I \rightarrow N_P < N_I$ is carried out under the same density. On the other hand, in the case of high densities, the situation is different. Under the above transformation, the flux and the order parameter do not change in parallel but flux increases while the order parameter decreases. The reason for this is that the high number of ImP positively affects lane formation, therefore, pedestrian mobility remains high despite high density and disorder.

Acknowledgments

The authors greatly thank Dr. Coskun Deniz for their support in conducting the characterization.

Authors' Contributions

In this study, TK created the idea, designed the structure, evaluated the characterized results, performed a literature review, produced the samples, completed experimental works, wrote up the article.

Competing Interests

The authors declare that they have no conflict of interest.

References

[1] Molnar P. Helbing D. Social force model for pedestrian dynamics. *Phys. Rev. E*, 51:4282, 1995.
[2] Vicsek T. Helbing D., Farkas I. Simulating dynamical features of escape panic. *Nature*, 407, 2000.
[3] Moldovan H. Parisi D. R., Gilman M. A modification of the Social Force Model can reproduce experimental data of pedestrian flows in normal conditions. *Physica A*, 388:3600, 2009.
[4] Chao G. Xiaoping Z., Wei L. Simulation of evacuation processes in a square with a partition wall using a cellular automaton model for pedestrian dynamics. *Physica A*, 389:2177, 2010.
[5] Löhner R. On the modeling of pedestrian motion. *Applied Mathematical Modelling*, 34:366, 2010.
[6] Schadschneider A. Chraibi M., Seyfried A. Generalized centrifugal-force model for pedestrian dynamics. *Phys. Rev. E*, 82:046111, 2010.
[7] Schadschneider A. Seyfried A. Chraibi M., Wagoum U.K. Force-based models of pedestrian dynamics. *Networks and Heterogeneous Media*, 692:425, 2011.
[8] Nishinari K. Schadschneider A., Kirchner A. From Ant Trails to Pedestrian Dynamics. *Applied Bionics and Biomechanics*, 1(11), 2003.
[9] Nishinari K. Schadschneider A. Chowdhury D., Guttal V. A cellular-automata model of flow in ant trails: non-monotonic variation of speed with density. *J.Phys. A*, 35:573, 2002.
[10] Schadschneider A. Nishinari K., Chowdhury D. Cluster formation and anomalous fundamental diagram in an ant-trail model. *Phys. Rev. E*, 67:036120, 2003.
[11] Chowdhury D. Nishinari K. John A., Schadschneider A. Collective effects in traffic on bi-directional ant trails. *Journal of Theoretical Biology*, 231:279, 2004.
[12] Rose G. Burd M. Shiwakoti N., Sarvi M. Enhancing the Safety of Pedestrians during Emergency Egress: Can We Learn from Biological Entities? *Transportation Research Record*, page 2137, 2002.
[13] Rose G. Burd M. Shiwakoti N., Sarvi M. Biologically Inspired Modeling Approach for Collective Pedestrian Dynamics under Emergency Conditions. *Transportation Research Record*, 2196:176, 2010.
[14] Francis L. W. R. Duncan E. J. Communication in ants. *Current Biology*, 16:570, 2006.
[15] Schadschneider A. Nowak S. Quantitative analysis of pedestrian counterflow in a cellular automaton model. *Phys. Rev. E*, 85:066128, 2012.
[16] Nishinari K. Suma Y., Yanagisawa D. Pedestrian dynamics: Modeling and experiment. *Physica A*, 391:248, 2012.
[17] Kayacan O. A theoretical model for uni-directional ant trails. *Physica A*, 390:1111, 2011.
[18] Kayacan O. Kunduracı T. A Monte Carlo study of ant traffic in a uni-directional trail. *Physica A*, 392:1946, 2013.
[19] Kayacan O. Kunduracı T. Uni-directional trail sharing by two species of ants a Monte Carlo study. *J. Stat. Mech.*, page P06038, 2015.
[20] Kayacan O. Gökce S. A cellular automata model for ant trails. *Pramana*, 80:909, 2013.
[21] Kayacan O. Gökce S. Study on bi-directional pedestrian movement using ant algorithms. *Chinese Phys. B*, 25:010508, 2016.
[22] Sun Y. Kinetic Monte Carlo simulations of bi-direction pedestrian flow with different walk speeds. *Physica A*, 549:124295, 2020.
[23] Hao Q. Y. et al. Phase behaviors of counterflowing stream of pedestrians with site-exchange in local vision and environment. *Physica A*, page 125688, 2021.
[24] You L. et al. A study of pedestrian evacuation model of impatient queueing with cellular automata. *Phys. Scr.*, 95:095211, 2020.
[25] Kretz T. Pedestrian Traffic, Simulation and Experiments, 2007. PhD. thesis.
[26] Löwen H. Rex M. Lane formation in oppositely charged colloids driven by an electric field: Chaining and two-dimensional crystallization. *Phys. Rev. E*, 75:051402, 2007.